



Creating virtual acoustic replicas of real violins

Esteban Maestre^{*}, Gary Scavone[†]

Computational Acoustic Modeling Laboratory
Centre for Interdisciplinary Research in Music Media and Technology
Schulich School of Music, McGill University, Canada

Abstract

We provide an overview of a current research project on measuring, modeling, and virtually recreating the sound radiation characteristics of real acoustic violins. Our general approach is based on measuring the directivity of an acoustic violin, and designing a digital filter structure that mimics the observed directivity while allowing interactive operation. The digital filter structure is fed by the electrical signal coming from a silent electric violin as played by a musician. In a hemi-anechoic chamber, we use a microphone array to characterize the frequency-dependent directivity transfer function of a real violin by exciting the bridge with an impact hammer and measuring the acoustic pressure at 4320 points on a sphere surrounding the instrument. From the input force and output pressure signals obtained from the real violin measurements, we use deconvolution to estimate 4320 impulse responses each corresponding to a radiation direction. With such impulse responses, we use State Wave Synthesis to model the observed directivity in time-varying conditions and efficiently render directional wavefronts in a virtual environment. We characterize the silent violin transfer function by exciting the bridge with an impact hammer and measuring the electrical signal at its output, leading to an impulse response that we use to design an inverse filter to recover the force excitation at the bridge.

Keywords: Violin, Radiation, Virtual, Replica, Directivity, Electric Violin, Silent Violin

1 INTRODUCTION

This research project is focused on the accurate characterization of the acoustic properties of traditional musical instruments and the development of digital models capable of efficiently reproducing such properties in interactive contexts. One application of this research is the preservation and virtual reproduction of historically valuable musical instruments, such that they can be played and heard in real time. Our project is motivated in part by the Stradivari *Messiah* violin, considered to be the most treasured masterpiece by this historic Cremonese maker because of its “as-new” condition but which has seldom been played and remains inaccessible, on display at the Ashmolean Museum in Oxford [1, 2]. Our objective is to develop methods for measuring, modeling, and virtually reproducing the acoustic radiation properties of real acoustic violins as a technological means for preserving and reproducing the acoustic properties of valued musical instruments (beyond performance recordings, pictures, or material and geometric data and analysis). This manuscript provides a brief overview of our progress so far.

There have been many reports of violin radiation pattern measurements in the past (a few of these include [3, 4, 5, 6, 7], with a good summary by [8]). In most cases, the measurements and analyses were made to evaluate and/or compare different instruments to one another. In [9], the authors use a frequency-domain approach to estimate directional frequency responses for later use in a sample-based sound synthesis system: glissandi are played on a violin in an anechoic chamber and the sounds are recorded for a discrete set of directions, from which frequency responses are estimated using frame-by-frame deconvolution of the harmonic tones. In our case, we capture a more comprehensive directivity frequency range by exciting the instrument with an impact hammer, and use a time-domain digital filtering method for simulating directivity. In the following, we report our developments on two main tasks: measurement and digital modeling of the acoustic radiation properties of a real violin, and measurement and digital modeling of the transfer function of an electric violin, with which a virtual acoustic replica of the real violin is to be virtually performed.

^{*}esteban@music.mcgill.ca

[†]gary@music.mcgill.ca



Figure 1. Semi-circular microphone array, rotating base, and support rig used to measure sound pressure signals at 4320 points on a one-meter-radius sphere around the violin. The laser Doppler vibrometer (on the tripod) was only used not used during the sound pressure measurements.

2 MEASUREMENT

2.1 Acoustic violin

In a similar fashion as performed for violin sound synthesis by digital waveguides [10], we define the frequency-domain radiativity transfer function of an acoustic violin by relating the force exerted by the strings on the bridge and the sound pressure radiated at a far-field distance from the instrument. Here, instead of considering a single external microphone position, we use a microphone array to measure the complete frequency-dependent directivity pattern on a sphere around the instrument, assuming far-field conditions.

In a hemi-anechoic chamber (with a carpeted floor and extremely low reflectivity), we carried out radiativity measurements on a violin from the Schulich School of Music at McGill University. The instrument was held vertically, with the neck pointing up, on a rotating base. Cushioned clamps were used in conjunction with a purposely machined shoulder rest to naturally fix the end of the body of the instrument to a vertical pole attached to the rotating base. Rubber bands were used to damp the strings. A semi-circular, one-meter-radius array of 60 high-precision, calibrated Sennheiser KE4-211-2 microphones was placed to cover 15/16 of elevation angle span of a sphere around the violin position, whose center was defined as the midpoint between the F-holes at an equal distance between the back and top plates. The measurement setup is shown in Figure 1. The laser Doppler vibrometer (Polytec LDV-100), mounted on the tripod, was used to initially measure the admittance of the violin but not for the subsequent radiativity measurements.

The impact hammer, which has been long used in the context of vibratory analysis or modeling [11, 12],

provides a simple and effective method to drive stringed instruments with great repeatability. For our measurements, a calibrated miniature impact hammer (PCB Piezotronics 086E80) was used to excite the corner of the bass side of the bridge in the direction corresponding to the horizontal transverse motion of the strings, parallel to the bow motion. The radiated sound, together with the hammer force, was measured by each of the 60 microphones for rotating base angle increments of 5 degrees, leading to $72 \times 60 = 4320$ signal measurement combinations. For each combination, three distinct measurements were made and later averaged. The spherical sector defined by the microphones covered 95% of the sphere. In our modeling framework, the strings are assumed to meet at a single point representing a common excitation position, so for practical matters, we could also have chosen to measure on the treble side. We chose to measure on the bass-bar side because of the higher efficiency of the bridge there in driving the top plate, as observed from previous experimental studies of violin acoustics [13]. Time-domain signals of force and sound pressure were collected, delay-compensated, and stored before using frequency-domain deconvolution to obtain directivity frequency responses. Signals were sampled at a rate of 48 kHz, and coherence analysis revealed strong consistency up to approximately 7 kHz.

2.2 Silent electric violin

We measured the response of a high-end commercially available silent electric violin, which we assume can be modeled as a linear, time-invariant system with a frequency response determined from input-output measurements. As with the acoustic violin, the strings were damped with rubber bands and the miniature impact hammer was used to excite the corner of the bass side of the bridge in the direction corresponding to the horizontal transverse motion of the strings. The electrical output signal provided by the violin was recorded simultaneously with the hammer force. Both signals were recorded at a sample rate of 48 kHz. By way of frequency-domain averaging over 3 distinct measurements, the frequency response of the electric violin was computed by deconvolution. Coherence analysis revealed strong consistency up to approximately 12 kHz.

3 ANALYSIS & MODELING

3.1 Acoustic violin directivity

We use State Wave Synthesis (SWS) [14] to model and simulate the frequency-dependent directivity of the acoustic violin. To do so, we design a mutable state-space model of 58 state variables, one non-mutable input (bridge excitation force) and an indefinite number of mutable outputs (sound pressure), each corresponding to an outwards direction expressed by two angles in vertical polar coordinates on a spherical coordinate system determined by the measurement sphere center. Assuming minimum-phase, a set of 58 common eigenvalues are estimated from the measured input admittance of the instrument. The specific number of eigenvalues was determined somewhat arbitrarily based on the quality of the frequency-domain fit. Alternatively, a similarly representative set of common eigenvalues could be obtained by performing modal analysis on a subset of the radiation measurements, though the input admittance tends to have a better signal to noise ratio. The output coordinate space of the output-mutable state-space model is defined as a bounded two-dimensional Euclidean space, with dimensions being the azimuth θ and elevation φ angles of the microphone measurement positions. In a first step, the state-to-output projection coefficients corresponding to the 4320 measurements are estimated by least-squares, leading to a matrix of 4320×58 projection coefficients. Then, estimated projection coefficients are arranged as 58 matrices of 72×60 entries each, to perform smoothing and re-sampling of the output coordinate space to obtain 58 matrices of 64×64 coefficients each (again, the specific size of the matrices is arbitrary). Finally, an output projection function is devised to perform bilinear interpolation of output projection coefficients over the space of output coordinates. Note that the mutable state-space model resulting from this modeling procedure can be equivalently expressed in real form by combining complex-conjugate pairs of eigenvalues into real second-order parallel sections whose numerator coefficients are provided by an output mapping function by bilinear interpolation. Example models of radiation frequency responses are displayed in Figure 2 along with their corresponding measured responses.

To demonstrate the dynamic behavior of the radiation model, we synthesize the input-output frequency re-

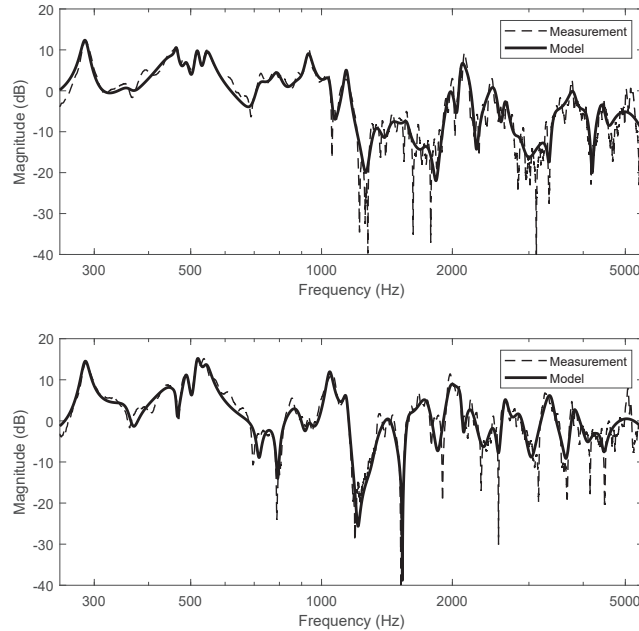


Figure 2. Detail of the radiation frequency response model. Input-output magnitude frequency responses of two individual measurements and their corresponding modeled responses, as obtained from the model. Top graph coordinates: azimuth $\theta = 1.97$ rad, elevation $\varphi = -0.21$ rad; bottom graph coordinates: azimuth $\theta = 1.02$ rad, elevation $\varphi = 0.26$ rad.

sponse as obtained from exciting the model in time-varying conditions. For 512 consecutive steps, we modify the output coordinates of an outgoing wave as captured by an ideal microphone lying on the sphere surrounding the source object. Assuming ideal excitation of the violin bridge, we simulate a continuous linear motion of the ideal microphone on the sphere, from initial position at ($\theta = 0.69$ rad, $\varphi = 4.71$ rad) to a final position at ($\theta = -1.48$ rad, $\varphi = -0.52$ rad). To illustrate the quality and smoothness of the achieved result, in Figure 3 we compare the measured frequency responses (nearest-neighbor) and the model frequency responses as obtained from bilinear interpolation of processed output projection coefficient vectors.

This modeling procedure, for which more details can be found in [14], allows the interactive simulation of the radiation properties of the acoustic violin given the time-varying position and orientation of the virtual instrument. To do so, the mutable state-space model is used to efficiently render multiple outgoing wavefronts representing the direct field and reflections, and propagating them to a listener in a virtual space. The frequency-dependent directivity of the listener, represented as a binaural HRTF, can be also simulated by a mutable state-space model as described in [14], with inter-aural time differences realized by fractional delay lines.

3.2 Electric violin equalization

In order to obtain an approximation of the bridge force signal $F(t)$ of the silent electric violin, which is needed to excite the radiation model, we “whiten” the electric violin output signal $E(t)$. This is achieved by using the electric violin transfer function measurement to design a matched minimum-phase, recursive parallel filter. As well, an inversion formula that preserves the parallel configuration of the designed filter is derived. First, a minimum-phase, magnitude-only specification technique is used to design an order-30 recursive parallel filter $H(z) = c + \sum_{m=1}^M H_m(z)$ comprising a real constant c and real-single or complex-conjugate poles spread over M parallel first-order sections $H_m(z) = r_m/(1 - p_m z^{-1})$ (the order M is arbitrarily determined based on quality of

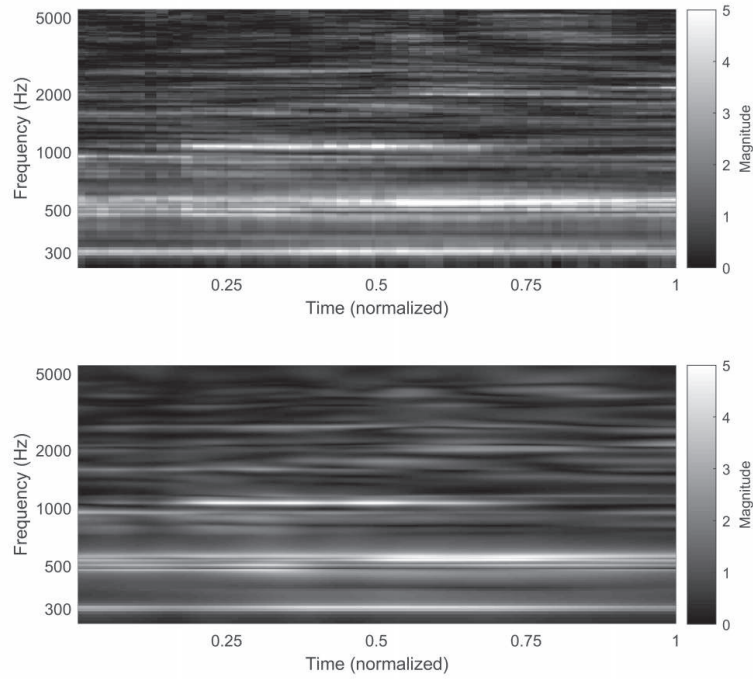


Figure 3. Input-output magnitude frequency response as obtained from exciting the radiation model in time-varying conditions: continuous linear motion of an ideal microphone on the sphere, from initial position at $(\theta = -0.69 \text{ rad}, \varphi = -0.34 \text{ rad})$ to final position at $(\theta = 5.06 \text{ rad}, \varphi = 1.39 \text{ rad})$. Top graph: nearest-neighbor measurement; bottom graph: bilinear interpolation of processed output projection coefficients.

the frequency-domain fit). Then, we express each $H_m(z)$ as $H_m(z) = r_m + z^{-1}G_m(z)$, with $G_m(z) = r_m p_m / (1 - p_m z^{-1})$. With this, the parallel filter $H(z)$ becomes $H(z) = g + z^{-1}G(z)$, where $g = c + \sum_{m=1}^M r_m$ and $G(z) = \sum_{m=1}^M G_m(z)$. Now it is possible to invert the transfer function $H(z)$ and obtain the input force signal $F(z)$ from the output electrical signal $E(z)$ via $F(z) = g^{-1}(E(z) - z^{-1}G(z)F(z))$ while preserving the parallel architecture. The resulting model and equalization are depicted in Figure 4.

4 OUTLOOK

The work reported here represents the early stages of a project intended to allow virtual acoustic rendering of acoustic violins (characterized from measured responses) using a silent electric violin. Complete measurements on a McGill-owned violin, as well as a Bergonzi from the Montreal area, have been performed. Subsequent use of less complete measurements (substantially lower number of external microphone positions, more reverberant room conditions, ...) of the Stradivari *Messiah* violin has previously been investigated [15] and is still under development. Other aspects of the project include the virtual reality rendering, motion tracking, room response modeling, perceptual testing with players and ultimately the staging of a performance demonstrating the resulting technologies.

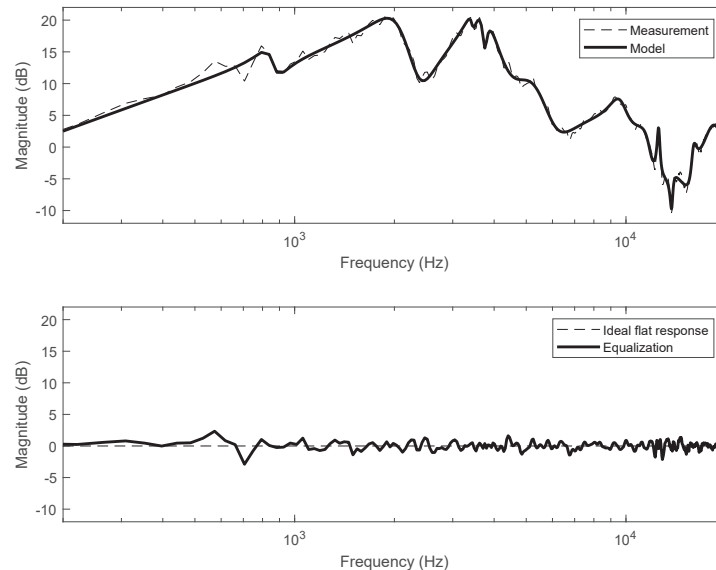


Figure 4. Silent violin digital equalization (full-band). Top graph: magnitude frequency response of the silent violin along with the response of a correspondingly designed order-30 recursive parallel filter. Bottom graph: magnitude frequency response of the equalized silent violin signal, as obtained from a parallel-inverted recursive filter.

ACKNOWLEDGEMENTS

We would like to thank Julius O. Smith for fruitful discussions on the digital filter structures and digital filter design methods applied in this work, and Harish Venkatesan for his assistance in the directivity measurements.

REFERENCES

- [1] <http://www.oxfordtoday.ox.ac.uk/features/caged-messiah>
- [2] <http://tarisio.com/cozio-archive/property/?ID=40111>
- [3] Meyer, J. Directivity of bowed stringed instruments and its effect on orchestral sound in concert halls. *Journal of the Acoustical Society of America*, Vol. 51 pp. 1994–2009. 1973.
- [4] Cremer, L.; Lehringe, F. Radiation of closed body surfaces. *Acustica*, Vol. 29 pp. 137–147. 1973.
- [5] Bissinger, G.; Keiffer, J. Radiation damping, efficiency, and directivity for violin normal modes below 4 kHz. *Acoustics Resesearch Letters*, Vol. 4, pp. 7–12. 2003.
- [6] Jansson, E. V.; Molin, N. E.; Sundin, H. Resonances of a violin studied by hologram interferometry and acoustical methods. *Physica Scripta*, Vol. 2(6), pp. 243–56. 1970.
- [7] Marshall, K. D. Modal analysis of a violin, *Journal of the Acoustical Society of America*, Vol. 77, pp. 695–709. 1985.
- [8] Woodhouse, J. The acoustics of the violin: a review. *Reports on Progress in Physics*, Vol. 77(11). 2014.

- [9] Perez-Carrillo, A.; Bonada, J.; Patynen, J.; Valimaki, V. Method for measuring violin sound radiation based on bowed glissandi and its application to sound synthesis. *Journal of the Acoustical Society of America*, Vol. 130(2), pp. 1020–1029, 2011.
- [10] Maestre, E.; Scavone, G. P.; Smith J. O. Joint Modeling of Bridge Admittance and Body Radiativity for Efficient Synthesis of String Instrument Sound by Digital Waveguides, *IEEE/ACM Transactions on Audio, Speech, and Language Processing*, Vol. 25 (5), pp. 1128-1139, 2017.
- [11] Jansson E. V. Admittance Measurements of 25 High Quality Violins, *Acta Acustica United with Acustica*, Vol. 83 (2), pp. 337-341, 1997.
- [12] Bissinger, G. Structural Acoustics Model of the Violin Radiativity Profile, *Journal of the Acoustical Society of America*, Vol 124 (6), pp. 4013-4023, 2008.
- [13] Alonso, J.; Jansson E. V. Input Admittance Eigenmodes and Quality of Violins, *Proceedings of the 103rd Meeting of the Acoustical Society of America*, pp. 60-75, 1982.
- [14] Maestre, E.; Scavone G. P; Smith ,J. O. Virtual Acoustic Rendering by State Wave Synthesis, *Proceedings of EAA Spatial Audio Signal Processing Symposium, Paris, France, 2019*.
- [15] Chafe, C.; Maestre, E.; Sarti, A.; Canclini, A.; Scavone, G.; Smith, J.; Antonacci, F. The Return of the Messiah: Modal Analysis and Bridge Admittance Modeling. *Proceedings of the 2017 International Symposium on Musical Acoustics, Montreal, Canada, 18-22 June, p. 70, 2017*.